8th Australasian Remote Sensing Conference, Canberra, 25-29 March, 1996

ON THE DETECTION OF VOLCANIC ASH IN NOAA AVHRR INFRARED SATELLITE IMAGERY

R.J.Potts and E.E.Ebert
Bureau of Meteorology
GPO Box 1289K, Melbourne, VIC

ABSTRACT

Satellite remote sensing techniques which can detect the presence of volcanic ash clouds in a timely manner offer the potential for improving warnings for volcanic ash clouds for the aviation industry. Studies have shown that areas where the brightness temperature difference, T4-T5, is negative on NOAA AVHRR satellite data can discriminate volcanic ash clouds from water/ice clouds, a problem in single channel satellite imagery. However, experience has shown that in the tropical Asia region negative differences can occur at very cold cloud top temperatures when no ash is present. These cases result in 'false alarms' and limit the scope for initial detection of a volcanic ash cloud based on satellite imagery. These negative differences can be largely explained by a failure to account correctly for non-linearities in the response of the radiometer at very cold temperatures, and by convective clouds which penetrate the tropical tropopause and which are capped by a strong temperature inversion at the top of the cloud layer.

INTRODUCTION

Satellite data have proved most valuable for monitoring the movement of volcanic ash clouds and providing operational warnings for the aviation industry. However, the discrimination of volcanic ash clouds from water/ice clouds is difficult and several studies have shown that advanced very high resolution radiometer (AVHRR) data from the NOAA polar orbiting satellites can improve this (Prata 1989a; Prata, 1989b; Holasek and Rose, 1991; Potts, 1993). Prata (1989a,b) demonstrated that areas where the brightness temperature difference between Channel 4 and Channel 5 (T4-T5) is negative may indicate the presence of volcanic ash whereas this difference is typically positive for water/ice clouds. There are limitations however. In a cloud which comprises a mixture of ash and water/ice particles or if an ice cloud overlies an ash cloud then negative differences may not be observed (Rose et al, 1995). Operational experience in Australia has also shown that negative differences can occur over tropical areas of Asia when no ash plume is present but there is deep convection and associated very cold cloud top temperatures. These "false alarms" reduce the operational efficacy of any warning system based on these satellite data and limit any possibility for automating the detection of volcanic ash clouds.

Fig.1. shows a scatter diagram of T4-T5 as a function of T4 for the NOAA 11 AVHRR pass of 2019 UTC, 23 March, 1994, across the Indonesia region, (image not shown). At this time there was no volcanic activity in the area and no volcanic ash was reported, yet there was an extensive and largely contiguous area where T4-T5 was negative. The scatter diagram shows an inverted parabola

characteristic of water/ice clouds; however it can be seen there are negative differences for brightness temperatures less than 220K which tend more negative as the brightness temperature gets colder. The lowest observed brightness temperature is 180K with an associated T4-T5 approximately -4.5K. A number of arguments have been suggested to explain the observed negative differences including pixel alignment of the scans for each channel, the viewing geometry (nadir vs off-nadir), refraction of sunlight into the sensors and electronic noise. In general these will have distinctive characteristics when viewed as an image and are easily identified. In this study we show that the observed "false alarms" can be largely explained by a failure to correctly account for the non-linear response of the AVHRR infrared sensors at cold temperatures and by overshooting cloud tops which penetrate the tropical tropopause. In this latter case we suggest a temperature inversion develops at the top of the cloud with the result that a negative value for T4-T5 is observed by the satellite rather than the

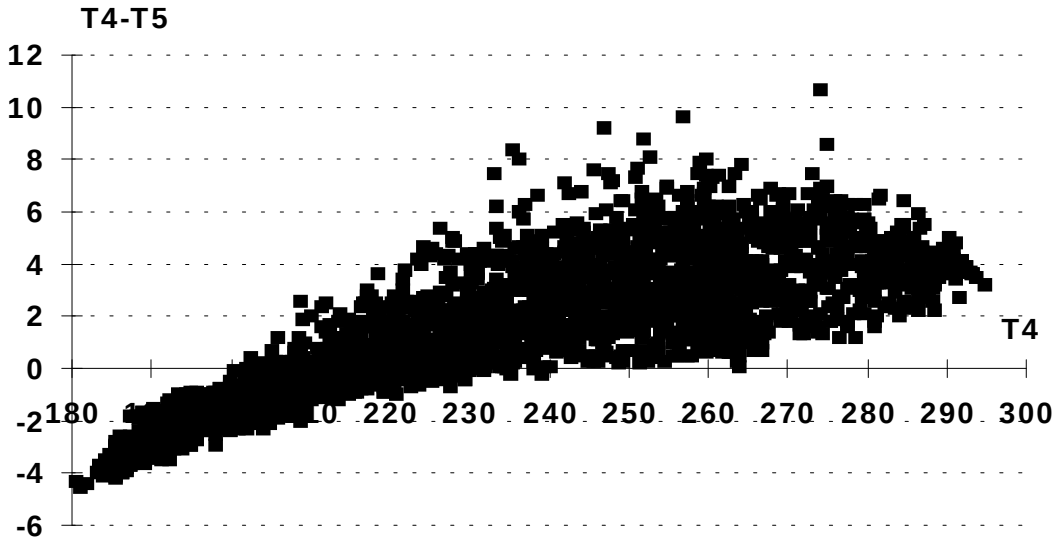

Figure 1. Scatter plot of T4-T5 (K) as function of T4 (K) for NOAA 11 AVHRR pass of 2019UTC, 23 March, 1994, over Indonesia region.

positive difference typically observed for water/ice clouds.

CALIBRATION OF AVHRR THERMAL CHANNELS

The NOAA AVHRR infrared channels are calibrated in-flight by viewing space and an internal calibrated target of known temperature and emissivity mounted in the instrument baseplate. For each scan line of the satellite pass the measured radiances for space, the internal target and the earth scan are digitised and transmitted together with the temperature of the internal calibrated target. The two calibration points provide sufficient information to enable the earth radiance to be determined from the output counts of the radiometer assuming the response of the radiometer is linear in the particular wavelength band (Planet, 1988; Kidwell, 1991). The brightness temperature is calculated from the radiance using the Planck equation. For Channel 3 the linearity assumption for the response of the radiometer is adequate, however for Channels 4 and 5, photoconductive HgCdTe detectors are used and these have a non-linear response. This non-linearity in Channels 4 and 5 can introduce errors of several degrees in the derived brightness temperature if not correctly accounted for (Brown et al,

1985).

Prior to the launch of NOAA14 the approach used by the NOAA National Environmental Satellite, Data, and Information Service (NESDIS), and described by Weinreb *et al*., (1990) was to apply a non-linear correction (NLC), determined in prelaunch laboratory tests, to the brightness temperature derived from the Planck equation. These non-linear corrections are published by NOAA NESDIS as Appendices to NOAA Technical Memorandum NESS 107, (Planet, 1988). Table 1 shows the published NLC's for NOAA 12. There is no allowance for any drift of these corrections with time. An important fact to note is that although original calibration tests were conducted for the temperature range 175-320K only corrections for the range 205-320K are published. Over the tropical Asia regions cloud top temperatures less than 205K are often observed and the correction made at these temperatures is dependent on the implementation in the system used to process and display these data.

The Bureau of Meteorology uses the McIDAS system (LeMarshall *et al*, 1987) for the processing and display of satellite data for both operational and research applications. This includes the routine processing of NOAA AVHRR satellite data for the detection and monitoring of volcanic ash clouds over the region to the north of Australia. Areas in the imagery where T4-T5 is negative are highlighted and subsequently identified as ash cloud if there have been any reports of a volcanic ash cloud or an eruption. In the McIDAS system the non-linear corrections to the AVHRR satellite data are made in accordance with the tables published in Planet (1988). For brightness temperatures equal to, or less than 205K the NLC corresponding to 205K is applied. The application of the NLC's in such a manner results in a negative bias to the brightness temperature difference, T4-T5, for brightness temperatures less than 205K and contributes to the incidence of "false alarms" in the detection of volcanic ash.

Table 1. Nonlinearity corrections for NOAA 12 AVHRR

	Channel 4. ICT (C)				**Channel 5.** ICT(C)			
Sc.Temp(K)	10	15	20	25	10	15	20	25
205	-1.58	-1.80	-1.31	-1.33	-1.17	-1.16	-1.19	-1.23
215	-1.24	-1.65	-1.49	-1.53	-1.15	-1.19	-1.17	-1.16
225	-1.33	-1.65	-1.58	-1.67	-1.01	-1.10	-1.15	-1.19
235	-1.05	-1.59	-1.51	-1.63	-0.88	-0.94	-1.01	-1.10
245	-1.18	-1.40	-1.58	-1.62	-0.63	-0.76	-0.88	-0.94
255	-1.04	-1.20	-1.53	-1.59	-0.47	-0.53	-0.63	-0.76
265	-0.71	-0.97	-1.19	-1.32	-0.37	-0.41	-0.47	-0.53
275	-0.41	-0.84	-1.05	-1.19	-0.21	-0.31	-0.37	-0.41
285	0.16	-0.23	-0.52	-0.70	0.08	-0.08	-0.21	-0.31
295	0.80	0.53	0.13	-0.16	0.37	0.18	0.08	-0.08
305	1.60	1.42	0.80	0.52	0.73	0.61	0.37	0.18
310	2.04	1.94	1.28	0.98	0.80	0.73	0.61	0.37
315	2.58	2.39	1.72	1.43	0.80	0.80	0.73	0.61
320	3.21	2.88	2.27	1.91	0.80	0.80	0.80	0.73

THE NON-LINEAR CORRECTION

As previously indicated the NLC is determined in prelaunch laboratory tests conducted by the ITT Aerospace/Optical Division. The AVHRR is located in a thermal/vacuum chamber, where it views a calibrated black body, representing the "Earth" scene; a black body cooled to 77K, representing the "Space" view; and the internal calibrated target (ICT). Data from the calibrated "Earth" target, the "Space" target and the ICT were recorded as the "Earth" target was cycled between 175K and 320K. The calibration procedure was carried out for a range of ICT temperature settings, (nominally 10, 15, 20 and 25C). Data were collected for "Earth" target temperatures in the range 175 to 320K though the NLC tables published by NOAA NESDIS only provide corrections for the temperature range 205 to 320K. Tables generated by ITT during calibration tests were obtained and the NLC's were recalculated in the same manner as described by Weinreb et al (1990), but for the temperature range 175-320K. Only results for NOAA 12 are presented here.

For Channels 4 and 5 the target radiances are computed from the measured temperature of the ICT, the "space" target and the "Earth" target as convolutions of the Planck function over the spectral response function for each sensor. The emissivity of the ICT, the "space" target and "Earth" target is assumed to be unity. Thus the radiance R is calculated by integrating the Planck blackbody function $B(\nu,T)$ across the channel response function $\phi(\nu)$:

$$R = \frac{\int_{\nu_1}^{\nu_2} B(\nu,T)\,\phi(\nu)\,d\nu}{\int_{\nu_1}^{\nu_2} \phi(\nu)\,d\nu} \qquad \textbf{(1)}$$

where ν_1 and ν_2 are respectively the lower and upper wavenumber limits for the response function as published by NOAA NESDIS. The integral is calculated numerically using Simpson's rule. The Planck function expressed in wavenumber space is:

$$B(\nu,T) = \frac{C_1 \nu^3}{e^{C_2 \nu / T} - 1} \qquad \textbf{(2)}$$

where $C_1 = 1.1910659.10^{-5}$ cm^3 mW/(m^2 sr cm^{-1}), and $C_2 = 1.438833$ cm K.

From the ICT temperature and measured radiance of the ICT and "space" target one can determine the "Earth" radiance, R_{lin}, based on a linear relationship;

$$R_{lin} = R_{IT}\frac{(x-SC)}{(IC-SC)} \qquad \textbf{(3)}$$

where x is the "Earth" target counts, SC is the "space" target counts and IC is the ICT counts registered by the radiometer. R_{IT} is the radiance for the ICT calculated from equation 1. From R_{lin}, the brightness temperature, T_{lin}, is determined using a temperature-radiance lookup table, previously calculated for temperature intervals of 0.1K using equations 1 and 2. The difference between the measured "Earth" target temperature, T_e, and T_{lin} is the correction to be applied to T_{lin}. The NLC's calculated in the manner outlined did not follow a smooth curve and Weinreb *et al*, suggests this is

due to inaccuracies in the experimental calibration procedures. A least squares cubic polynomial was therefore fitted to the data and the smoothed NLC's were determined for standard "scene temperatures".

NOAA 12

For NOAA 12 calibration tests were done by ITT at ICT temperatures of 10, 15, 20 and 25C. Table 2 presents a summary of the recalculated and smoothed correction terms ($\Delta T = T_e - T_{lin}$) for Channel 4 and 5 for each ICT temperature.

Table 2. Recalculated non-linear correction (K) for NOAA 12 AVHRR

	Channel 4. ICT(C)				**Channel 5**. ICT(C)			
Sc.Temp(K)	10	15	20	25	10	15	20	25
175	-0.33	-0.44	-0.57	-0.38	-1.76	-1.85	-1.63	-1.67
185	-0.69	-0.85	-0.84	-0.73	-1.54	-1.69	-1.46	-1.51
195	-0.98	-1.18	-1.08	-1.04	-1.34	-1.55	-1.32	-1.36
205	-1.19	-1.44	-1.28	-1.29	-1.18	-1.41	-1.19	-1.22
215	-1.33	-1.61	-1.44	-1.49	-1.03	-1.28	-1.08	-1.10
225	-1.39	-1.70	-1.54	-1.61	-0.89	-1.14	-0.98	-0.98
235	-1.36	-1.69	-1.58	-1.67	-0.75	-1.00	-0.87	-0.86
245	-1.24	-1.58	-1.54	-1.64	-0.61	-0.85	-0.75	-0.74
255	-1.02	-1.37	-1.40	-1.52	-0.45	-0.69	-0.62	-0.62
265	-0.70	-1.05	-1.17	-1.30	-0.28	-0.50	-0.46	-0.49
275	-0.27	-0.61	-0.83	-0.98	-0.08	-0.29	-0.27	-0.34
285	0.26	-0.05	-0.36	-0.54	0.16	-0.05	-0.05	-0.18
295	0.91	0.64	0.24	0.02	0.44	0.23	0.22	0.00
305	1.68	1.45	0.98	0.71	0.76	0.54	0.54	0.21
310	2.11	1.91	1.41	1.10	0.95	0.71	0.73	0.32
315	2.58	2.41	1.88	1.54	1.15	0.90	0.92	0.44
320	3.07	2.94	2.39	2.00	1.37	1.09	1.14	0.57

DETECTION OF VOLCANIC ASH

The impact of the NLC's on the derived value of T4-T5 can be illustrated by taking the difference in these corrections, ie., $\Delta T_4 - \Delta T_5$. Fig.2 and Fig.3 show $\Delta T_4 - \Delta T_5$ for NOAA 12 as a function of T4 for the published NLC's (Table 1) and recalculated NLC's (Table 2) respectively. In general the difference T4-T5, is less than 10K and often less than 3K. It is clear that if the NLC's are not accounted for when calculating T4-T5 significant errors may result. It is also evident that for brightness temperatures less than 205K a negative bias of up to 1.5K will result if the true NLC is not accounted for. This negative bias can partially explain the negative differences observed at the cold brightness temperatures seen in Fig.1, although it is not sufficient to fully account for the observed differences.

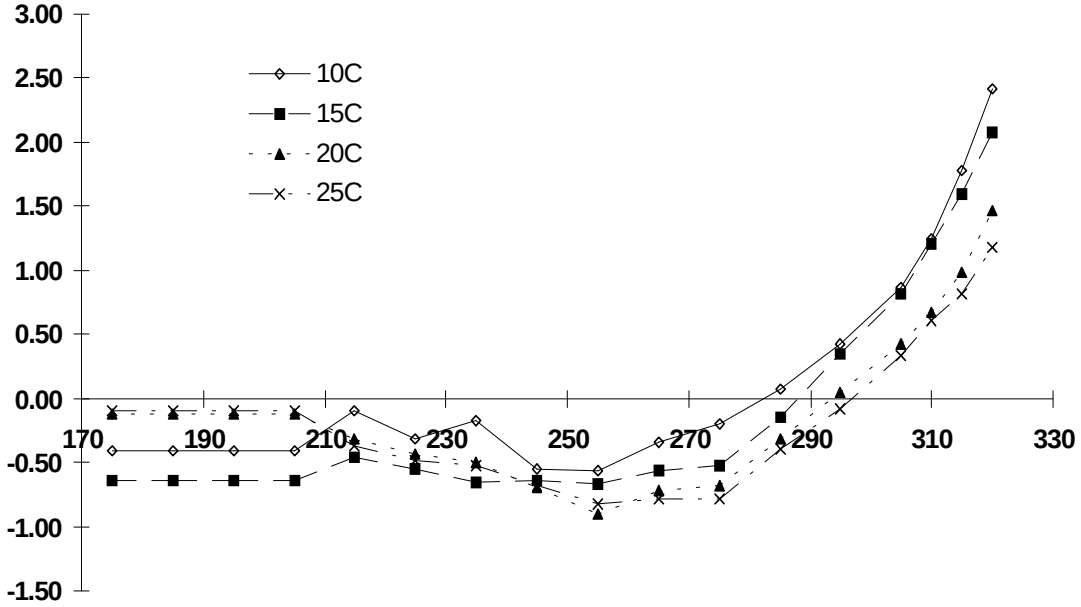

Figure 2. Difference in published NLC's (ΔT4-ΔT5) for NOAA 12 AVHRR for different values of ICT temperature.

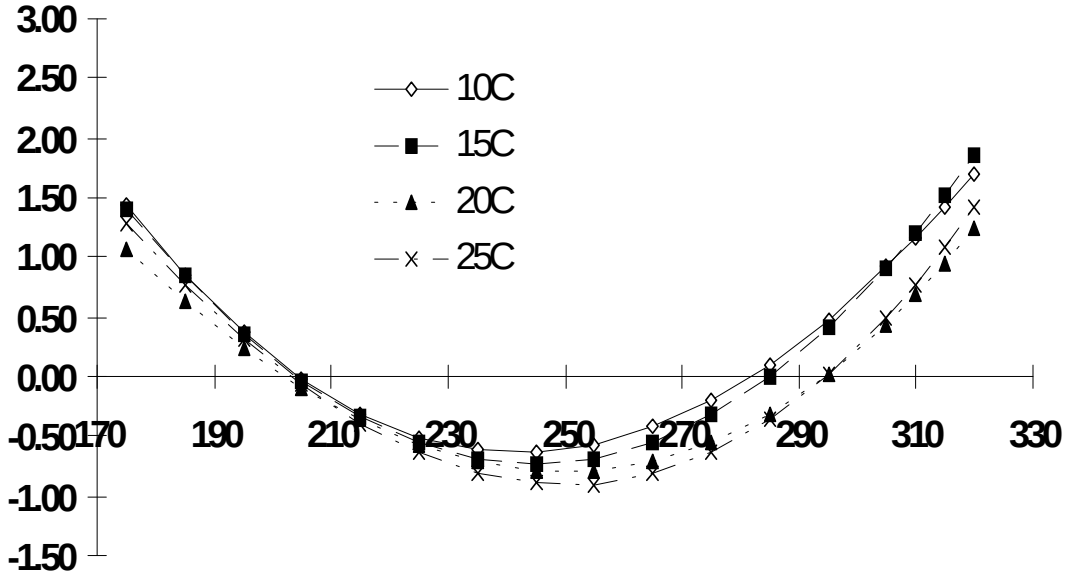

Figure 3. Difference in recalculated NLC's (ΔT4-ΔT5) for NOAA 12 AVHRR for different values of ICT temperature.

OVERSHOOTING DEEP CONVECTION

Positively buoyant saturated air within a storm updraft cools at the moist adiabatic lapse rate, gaining momentum as it ascends. If the upward momentum of the air parcel is large the air can penetrate the tropopause and rise well into the stratosphere. Continued cooling of the parcel can lead to extremely cold cloud brightness temperatures; values as low as 173K have been observed in clouds in the Western Pacific (Ebert and Holland, 1992). A steep temperature inversion exists at the cloud upper boundary, similar to that found at the top of inversion-capped boundary layer stratus clouds. In such a situation the T4-T5 signature could be negative if the majority of the radiation at 11.9 μm (Channel 5) emanates from a higher level, at a warmer temperature, than the radiation at 10.8 μm (Channel 4). This would lead to a "false alarm" suggesting the presence of volcanic ash when in fact there is none.

To test the possibilty that "false alarms" could be due in part to the thermal signal from overshooting deep convection, we performed simulations with a simple model using varying cloud structural and microphysical conditions. The simulations were conducted for the case shown in Fig.1, using a model of a storm updraft penetrating a stable lower stratosphere, as illustrated in Fig.4. It rises until it is no longer buoyant and the cloud has reached its maximum height, z_c. The upper portion of the cloud contains an inversion layer of thickness z_c-$z_{b,}$ and temperature differential, T_c-T_b. T_b represents the coldest temperature attained by the cloudy air during its ascent, and T_c is the temperature of the stratospheric environment at level z_c.

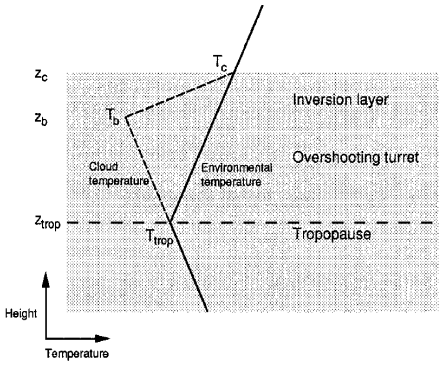

Figure 4. Temperature profile in overshooting cloud top.

The cloud is assumed to be composed of small spherical ice crystals of constant radius r and ice water content, IWC. Although neither r nor IWC would be constant in natural clouds, it is sufficient to treat them as such in order to explore the range of T4-T5 signatures associated with variations in cloud characteristics. If we further assume that the overshooting convection can be treated as a plane parallel homogeneous layer with negligible longwave scattering, then the upwelling radiance, *I*, seen by a downward looking satellite instrument at a given wavelength is given by the radiative transfer equation,

$$I = \tau B(T_{trop}) + \int_{z_{trop}}^{z_c} B(T,z)\frac{d\tau}{dz}dz \qquad \textbf{(4)}$$

where τ is the transmissivity of the layer and B(T,z) is the Planck function. The transmissivity is an exponential function of the extinction coefficient, β_{ext}, and the thickness of the layer,

$$\tau = e^{-\beta_{ext}(z_c - z_{trop})} \qquad \textbf{(5)}$$

The extinction coefficient depends on the extinction efficiency, Q_{ext}, which is a function of particle size. For a cloud composed of single size crystals the extinction coefficient can be expressed as

$$\beta_{ext} = \frac{3 Q_{ext} IWC}{4 \rho_i r} \qquad \textbf{(6)}$$

where ρ_i is the density of ice, specified as 0.9 g.cm^{-3}. Values of Q_{ext} for spherical ice crystals have been calculated by Prata (1989b) for wavelengths of 10.8 μm and 11.9 μm, which approximate the central wavelengths of AVHRR channels 4 and 5.

The temperature profile measured at 2300 UTC on 23 March 1994 at Darwin Airport was used to specify the stratospheric temperatures in the model. The tropopause temperature, T_{trop}, was 190K at an approximate altitude of 18 km. To cool enough to produce the observed minimum cloud brightness temperature of 182K the cloudy air would need to have risen at least 0.8 km above the level of the tropopause. We compute radiances for a variety of cloud conditions, which are then inverted using the Planck function (eq.2) to obtain the brightness temperatures T4 and T5.

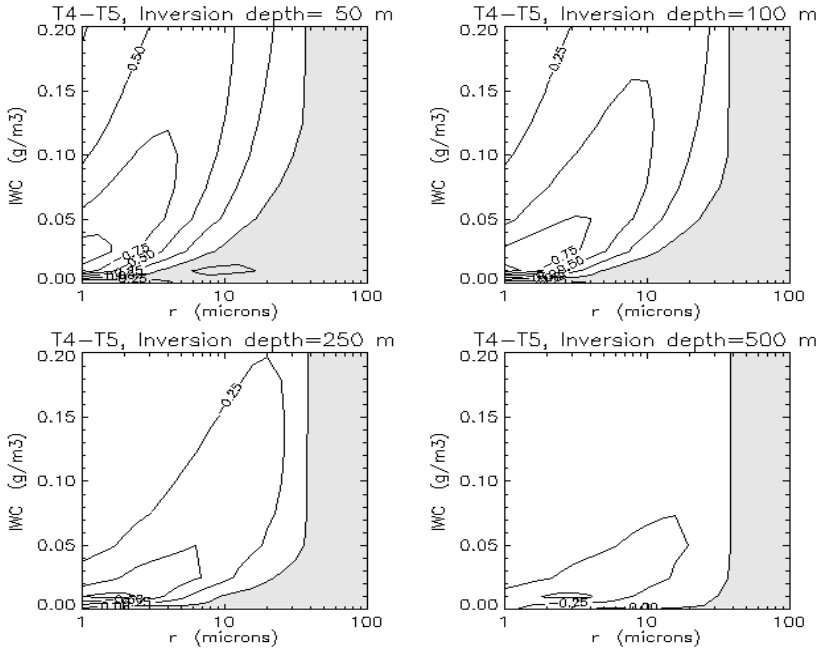

Figure 5. T4-T5 as function of particle radius and ice water content (see text).

Figure 5 shows contour plots of T4-T5 as a function of r, IWC, and inversion thickness for an overshoot depth of 1 km. Negative values of T4-T5 are produced for small crystal sizes and moderate values of IWC, i.e., those values which combine to produce large values of longwave extinction. This means that the radiances emanate from the inversion layer itself, with very little coming from the layer below the inversion. The negative T4-T5 difference is greatest when the effective source for 11.9 μm radiance is vertically distanced from the source of 10.8 μm radiance but both are in the inversion layer. For 1 km overshoot this value of T4-T5 ≃ -1.2K occurs for a crystal radius of 1.0 μm and IWC of 0.02 g.m^{-3}.

CONCLUSION

Remote sensing techniques which can detect the presence of volcanic ash clouds in a timely manner offer the potential for improving warnings for the aviation industry. Previous studies have shown that a negative brightness temperature difference, T4-T5, on NOAA AVHRR satellite data can indicate the presence of volcanic ash. Experience has shown that in the tropical Asia region negative differences can occur at very cold cloud top temperatures when no ash is present. These cases result in 'false alarms' and limit the scope for initial detection of a volcanic ash cloud based on satellite imagery. It has been shown that the negative differences can be largely accounted for by a failure to account correctly for non-linearities in the response of the radiometer at very cold temperatures and by convective clouds which penetrate the lower stratosphere.

ACKNOWLEDGEMENTS

The supply of the ITT calibration data by Dr Alistair Steyn-Ross is gratefully acknowledged.

REFERENCES

Brown O.B., Brown J.W., and Evans R.H., 1985: Calibration of Advanced Very High Resolution Radiometer Infrared Observations. J.Geophys.Res., 90, 11,667-11,677.

Ebert E.E., and Holland G., 1992: Observations of record cold cloud-top temperatures in Tropical Cyclone Hilda (1990). Mon.Wea.Rev., 120, 2240-2251.

Holasek R.E., and Rose W.I., 1991: Anatomy of 1986 Augustine volcano eruptions as recorded by multispectral image processing of digital AVHRR weather satellite data. Bull.Volcanol., **53**, 420-435.

Kidwell K.B., 1991: NOAA Polar Orbiter Data Users Guide. NOAA Satellite Data Services Division. Washington DC.

LeMarshall J.F., Stirling L.J., Davidson R.F., and Hassett M.J., 1987: The Australian Region McIDAS. Aust.Met.Mag., 35, 55-64.

Planet W.G., 1988: Data Extraction and calibration of TIROS-N/NOAA radiometers. NOAA Technical Memorandum NESS 107. NOAA National Environmental Satellite Data and Information Service. Washington DC.

Potts R.J., 1993: Satellite observations of Mt Pinatubo ash clouds. Aust. Met. Mag., 42, 59-68.

Prata A.J., 1989a: Observations of volcanic ash clouds in the 10-12 μm window using AVHRR/2 data. Int.J.Remote Sensing, 10, 751-761.

Prata, A.J., 1989b: Infrared radiative transfer calculations for volcanic ash clouds. Geophys. Res. Lett., 16, 1293-1296.

Rose W.I., Delene D.J., Schneider D.J., Bluth G.J.S., Krueger A.J., Sprod I., McKee C., Davies H.L., and Ernst G.G.J., 1995: Ice in the 1994 Rabaul eruption cloud: Implications for volcano hazard and atmospheric effects. Nature, 375, 477-479.

Weinreb M.P., Hamilton G., and Brown S., 1990: Nonlinearity corrections in calibration of Advanced Very High Resolution Radiometer infrared channels. J.Geophys.Res., 95, No.C5, 7381-7388.